Time-of-Flight Measurement Techniques for Airborne Ultrasonic Ranging

Joseph C. Jackson, Rahul Summan, *Student Member, IEEE*, Gordon I. Dobie, *Member, IEEE*, Simon M. Whiteley, S. Gareth Pierce, and Gordon Hayward, *Fellow, IEEE*

***Abstract*—Airborne ultrasonic ranging is used in a variety of different engineering applications for which other positional metrology techniques cannot be used, for example in closed-cell locations, when optical line of sight is limited, and when multipath effects preclude electromagnetic-based wireless systems. Although subject to fundamental physical limitations, e.g., because of the temperature dependence of acoustic velocity in air, these acoustic techniques often provide a cost-effective solution for applications in mobile robotics, structural inspection, and biomedical imaging. In this article, the different techniques and limitations of a range of airborne ultrasonic ranging approaches are reviewed, with an emphasis on the accuracy and repeatability of the measurements. Simple time-domain approaches are compared with their frequency-domain equivalents, and the use of hybrid models and biologically inspired approaches are discussed.**

I. Introduction

The accurate estimation of distance through time-of-flight (TOF) measurements is fundamental to a wide variety of engineering applications. For example, spatial localization is integral to industrial and research fields such as mobile robotics [1], location-aware sensor networks [2], asset tracking [3], and map building [4]. A major application for this research is in nondestructive evaluation using mobile robotics [1], in which accurate localization is needed to generate robot inspection paths to ensure uniform sensor coverage and to ensure the precise location of each measurement for subsequent fusion of different measurements sets. The location of an object can be calculated using distance measurements from three or more fixed landmarks. The accuracy of the location estimate is a function of the distance uncertainty, which is, in turn, a function of the uncertainty in the TOF measurement.

Ultrasonic-based airborne measurement systems have various advantages over other techniques such as visual techniques (e.g., multi-camera object tracking [5]), radio-frequency techniques (e.g., Global Positioning System (GPS) [6]), and optical techniques (e.g., laser trackers [7]). For instance, localization using ultrasonic techniques is typically inexpensive, and suitable ultrasonic sensor modules can be produced for as little as $10 each [8]. Such modules can be made very small, making them suitable for applications in miniature robotics. Ultrasonic ranging systems can also be used in electromagnetically shielded environments where other techniques, such as GPS, cannot be used.

Furthermore, the small footprint and low cost of ultrasonic sensor modules make them well suited for robot-mounted ranging and mapping [9]. Unlike positional systems that measure the TOF flight between two modules, ranging sensors measure the TOF of ultrasonic echoes and estimate the distance to a reflector. Algorithms such as simultaneous localization and mapping (SLAM) [9] are typically used to collate a series of these measurements into a map of the environment. Ultrasonic ranging sensors are potentially more accurate than laser-based devices such as miniature laser range-finders [10] which suffer from errors resulting from variations in the reflector's surface properties [11].

Material characterization is another important application of ultrasonic TOF measurement. Material geometries can be determined by reflecting an ultrasonic wave off the back-wall boundary and calculating the TOF. If the sample contains inhomogeneous regions, such as cracks or voids, these can often be located. Elsewhere, ultrasonic TOF techniques are used for biomedical imaging, structural health monitoring, and acoustic microscopy, among many others [12].

Most airborne ultrasonic measurement techniques employ the following concept: an acoustic signal is sent from a transmitter and travels through air to a receiver [12]. The TOF (t_F) for the signal to travel between transmitter and receiver can be used to calculate the distance between the ultrasonic transducers. The TOF (t_F) relates to the distance d between these two points and the speed of sound in the medium c through the simple equation $d = ct_F$. This is valid for pitch–catch methods, in which the receiver and transmitter are independent. Clearly, for pulse–echo methods, in which a single transducer both emits and receives, the range is $d = ct_F/2$. An accurate and repeatable measurement of the TOF is therefore crucial. Errors in this measurement can occur, however, because of the method of measuring the time delay between the transmitted and received signals.

This paper reviews the current state-of-the-art in acoustic airborne ranging algorithms, including simple thresholding techniques and cross-correlation, and includes the authors' investigations into phase-based chirp methods in the Fourier domain and a biologically inspired ranging algorithm.

Manuscript received October 25, 2011; accepted November 13, 2012. The authors acknowledge the Engineering and Physical Sciences Research Council (EPSRC) for their support of this work through the grants EP/C523776/1, EP/F017332/1, and EP/H02848X/1.

The authors are with the Centre for Ultrasonic Engineering, Royal College Building, University of Strathclyde, Glasgow, UK (e-mail: joseph.jackson@strath.ac.uk).

DOI http://dx.doi.org/10.1109/TUFFC.2013.2570

The central goal in choosing a measurement technique is to maximize both accuracy and repeatability. The meaning of these two terms is frequently confused, especially colloquially, because there is some degree of overlap in their definitions. Accuracy is defined here as the error between the actual and the measured value (or the mean of a set of measured values). Repeatability is defined as the standard deviation (or variance) of repeated measurements. In this context, repeatability is more likely to be affected by noise in any non-biased measurement system. Both accuracy and repeatability define different properties of any set of measurements and, as such, provide different levels of confidence about how well a measurement system performs. High repeatability reduces the need for averaging, because the error in a single measurement will be small—the value of a TOF measurement will not be significantly improved through repeated experiments. This property can be very important in, for example, robot positioning, in which the current position calculated from the TOF is often used in algorithms that control the motion of a robot, and hence refresh rates for the present position can significantly affect performance. A high level of accuracy simply tells us that the measurement is close to the real value. Note that repeatable measurements can be inaccurate, and vice versa.

Therefore, for ultrasonic TOF measurements, a high level of repeatability is desirable to reduce the time taken to be confident of the measurement. Accuracy, however, can suffer greatly from inherent biases in a chosen measurement system, whether from the TOF measurement itself, the value for the speed of sound in the medium, or both.

II. Time-Domain Methods

There are a multitude of different methods for calculating the TOF of an acoustic signal, and many have been studied in depth (for example, see [13]). The following subsections represent the general techniques that are commonly used.

A. Threshold Detection

The simplest form of measuring the TOF involves transmitting and detecting the arrival of an ultrasonic acoustic wave by triggering the event when the receiver voltage exceeds some predetermined threshold (see Fig. 1). The signal can be a single-frequency amplitude-modulated signal, or an impulse (which will be modified by the transducer frequency response and properties of the propagation channel). In general, transmitted signals are tone-bursts—several cycles of a single frequency, often windowed to optimize spectral content. Thresholding systems are usually used in conjunction with narrow-bandwidth transducers, which are generally more powerful than wideband transducers, and so have a greater range. A typical signal of this type can be seen in Fig. 1(top).

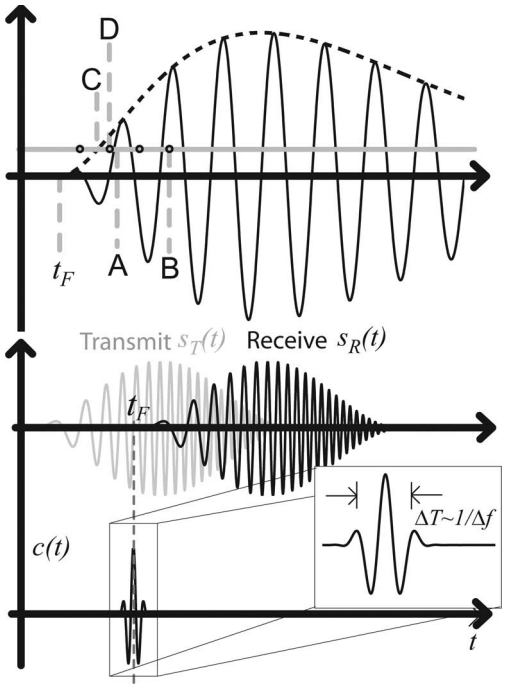

Fig. 1. (top) Errors in the threshold detection method for a narrowband signal (after [14]). Circles indicate hypothetical sampling for a case in which the sampling frequency is low. The gray line is a hypothetical threshold. (bottom) Cross-correlation with broadband linear chirps.

There are some advantages to this method. It does not typically require any complex computations and therefore can be achieved with simple circuitry. It can be implemented with inexpensive single-frequency ultrasonic transducers, further reducing cost. As a measurement technique it is, however, error-prone. Given certain hardware limitations, three problems may exist: low sampling frequency, low signal-to-noise ratio (SNR), and inherent bias. The first two problems are, in fact, common to all TOF techniques, and in this article all methods are reviewed or tested for their suitability and robustness by comparing their behavior in conditions with poor SNR.

Noise can increase the likelihood of false positives and threshold mechanisms are particularly susceptible to this type of error. In low-SNR environments, it is necessary to perform some form of amplification or, equivalently, reduce the threshold for detection, making it more likely that false positives occur as the threshold level and noise level become comparable. The effect of low sampling frequency is more subtle and is implicated in all time-domain methods: low sampling frequency decreases the resolution with which one can determine the time at which an event (such as a threshold being crossed) occurred. In the case of a threshold system, a low sampling frequency will always introduce a bias that can increase the measured delay (see Fig. 1).

Finally, there are two causes for an inherent bias to longer delays, independent of those mentioned, in a simple threshold system. First, no matter how ideal is the emitted pulse from the transducer, there will always be a rise time for the signal when it is detected. Second, and more

importantly, the decision of where to set the threshold is a compromise that introduces bias. As mentioned previously, a threshold set too low incurs too many false positives; indeed, typical thresholds are set at between 3 and 5 times the background noise level [13]. The major flaw in the threshold concept is that it inherently tries to measure the arrival time of a pulse, which for all real pulses is indistinguishable from the background noise (Fig. 1). Theoretically, an impulse signal combined with a threshold system would be an excellent method for TOF measurements. Because threshold detectors tend to incorporate narrowband transducers, however, and air itself acts as a low-pass filter [15], only narrowband signals can be transmitted. Furthermore, a narrowband receiver will respond more slowly to an incoming acoustic signal than a wideband receiver. Therefore, in setting the threshold to be at a level at which the receiver voltage is significantly above the noise floor, the result measured is delayed from the true TOF. This delay is never constant for all practical contexts, and so cannot simply be accounted for as a known offset. Fig. 1 indicates the process of thresholding and some of the associated problems, as the method can return delays at A and B, delayed from the true TOF t_{F}.

Many authors have dealt with these issues, usually retaining the desire for affordable solutions and minimal computation while still reducing error. For example, for an oscillatory signal, a threshold detector might miss the first detectable cycle of the signal if the sampling frequency is too low, noise is large, the threshold is set too high, or a combination of all three (Fig. 1). This problem can be reduced by extracting the envelope from the signal through rectification and low-pass filtering, and then performing a thresholding method. Bias in this type of thresholding system has been studied [14] and also extended to 2-D environments—the effect of a missed cycle is removed but the bias with respect to the threshold level still remains (Fig. 1, points C and D). A detailed study by Barshan [13] indicates that errors in a thresholding method sampled at 500 kHz for a range of 50 cm are ∼5 mm (accuracy) and ∼800 μm (precision) at an SNR of 35 dB. Note that, in general, most studies focus on the accuracy of a *distance* measurement, and therefore quote their results in meters. The accuracies quoted in this article continue this trend.

Other methods exist for extracting the envelope, including creating an *analytic signal* via the Hilbert transform [16]. In an attempt to locate the hidden start of the pulse, curve-fitting techniques have also been used [14], [17]. In these cases, the effects of bias can be ameliorated or removed completely by sampling two or three points and inferring from their distribution the time of the beginning of the pulse; for example, a parabolic fit is a reasonable approximation of a rising pulse [13], [14], [17]. Another example for improved thresholding is called the sliding-window method—a form of double-thresholding designed to reduce the appearance of false positives [13]. Rather than straightforward thresholding, this method counts the number of supra-threshold samples in a given window, which slides along the data series. When the number of supra-threshold samples itself exceeds a threshold, then the event is indicated to have occurred. This technique can reduce the effect of noise spikes and therefore allow a reduced threshold to exist, reducing bias.

B. Cross-Correlation

Cross-correlation is arguably the optimal TOF method [18]. In ultrasonic TOF systems, a cross-correlation between a transmitted signal and a received signal results in a peak at the delay time and a reduction in the noise level. Cross-correlation is also improved through signal design; a frequency-modulated signal will produce a narrower cross-correlated peak (Fig. 1) than that obtained by a single-frequency tone-burst. For these reasons, cross-correlation has been called *matched filtering*, and when used in conjunction with frequency-modulated signals, *pulse compression*. At its most simple, the method of cross-correlation takes a transmitted and received signal [$s_{\mathrm{T}}(t)$ and $s_{\mathrm{R}}(t) \sim s_{\mathrm{T}}(t - \tau_0)$] and produces a time-domain signal whose maximum occurs at the delay time τ_0. This cross-correlation $c(t)$ is calculated for these real signals by

$$c(t) = \int_{-\infty}^{\infty} s_{\mathrm{T}}(\tau) s_{\mathrm{R}}(t + \tau) \mathrm{d}\tau. \tag{1}$$

It is often simpler in practice to perform the calculation in the Fourier domain, where $C(f) = S_{\mathrm{T}}^{*}(f) S_{\mathrm{R}}(f) = \mathcal{F}(s_{\mathrm{T}}(t))^{*} \mathcal{F}(s_{\mathrm{R}}(t))$, and $c(t)$ is the inverse Fourier transform of the cross-spectrum $C(f)$. Cross-correlation has noise-reduction properties, because the cross-correlation of random noise is theoretically zero, so additive noise is reduced with cross-correlation.

1) Narrowband Signals: For narrowband signals, cross-correlation results in a narrowband waveform, and errors in determining the maximum can exist [19]. In particular, undersampling can be problematic in determining the true TOF, especially when the sampling frequency is decreased toward the Nyquist limit. Temporal methods for reducing this effect include parabolic curve fitting to a few data points around the peak (e.g., [20]), or upsampling the data. Typical values for errors in ranging over distances 10 to 90 cm are on the order of ∼2 mm (accuracy) and ∼1 mm (repeatability) when measuring just the TOF through correlation [20]. Parrilla *et al.* [16] simulated various methods and found an accuracy error for correlation on the order of 100 μm for sampling frequencies over a range of 3 to 11 times the signal frequency. Another study [13] quotes <5 μm accuracy error and <300 μm repeatability error over a range of 50 cm sampled at 500 kHz, and includes a detailed error analysis. Noise can also cause problems, because the narrowband signal will consist of several cycles at the signal frequency, and these adjacent cycles can be very similar in magnitude—noise can create false positives out of these adjacent peaks.

2) Frequency-Modulated Signals: Chirps: Cross-correlation will have increased accuracy when the waveform is not a single-tone signal but a frequency-modulated signal (FM), such as a linear chirp (Fig. 1). Cross-correlation of transmitted $[s_T(t)]$ and received chirps $[s_R(t)]$ produces a pulse whose maximum exists at t_F. The width of this pulse (ΔT) is inversely proportional to the bandwidth of the chirp (Δf); therefore, echoes are more easily separable with wideband chirps (Fig. 1). Therefore, not only does one obtain a distinct peak marking the delay, but closely spaced echoes can also be observed, provided they are separated in time by more than the width of the cross-correlated pulse, even though the echoes may overlap considerably in the original signals (Fig. 3).

Chirps are widely used in conjunction with cross-correlation for radar and sonar applications. They implicitly require wideband transducers, and if appropriate wideband technology is available, then cross-correlation using chirps is considered an optimal ranging method for detecting a known analog waveform in random white noise [18]. It is even thought that nature recognizes this, with evidence that echolocating bats perform a correlation-type process [21], [22], although the calls of bats are more complex than linear chirps, and often contain multiple higher harmonics.

III. Fourier-Domain Phase-Based Methods

If the capability exists for sampling and analyzing both the transmitted signal and the entire received signal, some benefit can be derived from transforming the time-series data to the Fourier domain. It is possible to extract the TOF from the phase of the frequency of both the transmitted and received signals. Fourier methods can make the TOF measurement, via the phase, more robust and accurate than temporal measurements. Further extensions to this idea include using multiple-frequency signals and frequency-modulated chirps, depending on application and the ultrasonic bandwidth that is available.

A. Single-Frequency Signals

Phase can be measured directly from a single-frequency signal and, from this, the TOF can be inferred. A simple description of a monotonic wave $s(x,t)$ at a spatial position x and time t, in a nondispersive medium, can be written, in complex form, as

$$s(x,t) = Ae^{i(kx-2\pi ft)} = Ae^{i(2\pi f((x/c)-t))}, \tag{2}$$

where A represents an amplitude, k is the wavenumber, f is the frequency of the signal, and c is the speed of sound in the medium. From (2), it is clear that at any point x, the Fourier transform of $s(x,t)$ results in a spectrum in which the phase ϕ of the frequency f is given by $\phi = 2\pi fx/c$. Note that the whole time record beginning at the start of transmission is required, or the phase will include an offset, rendering the result incorrect, because phase is a function of both time and space. Because x/c is explicitly the TOF t_F, the phase is a direct measure of the TOF. Phase is restricted mathematically, however, to only a 2π range, and therefore for any TOF $t_F > 1/f$, there exists ambiguity. In the context of ranging in air, this ambiguity occurs at very small distances, i.e., if $f = 40$ kHz and $c = 345$ ms^{-1}, then ambiguity occurs for any distance between transmitter and receiver greater than ~8.6 mm. Practically, therefore, a single-frequency phase method cannot work for large-scale TOF measurements in air, unless coupled with other methods. In the literature, this technique is often referred to as the phase-shift method [23].

B. Multi-Frequency Signals

An improved unambiguous range can be found by using two or more frequencies in a transmitted signal [23], [24]. There are two ways to visualize exactly why this method works, and there are advantages in this method derived from physical considerations (e.g., transducer properties). For the single-frequency method to work unambiguously over longer timescales (larger distances for the specific application of ranging), the frequency must be reduced. For example, to measure a distance that is from 0 to 345 mm away from the sensor in air (if $c = 345$ ms^{-1}), a signal with a frequency ~1 kHz must be used. This frequency is often not practical however, not least because it is audible, and longer distances require lower frequencies still. It is possible however to use two-tone signals, for example 40 and 41 kHz, and it can be shown that the *difference* in the phases of each tone is unambiguous for $x = c\Delta f \sim 345$ mm in air. Using two frequencies f_1 and f_2, one can derive an equation for the TOF t_F calculated as a function of the two frequencies' phases φ_2 and φ_1:

$$\begin{aligned} t_F &= \frac{1}{\Delta f}\left(\Delta n + \frac{\Delta\varphi}{2\pi}\right) \\ &= \frac{1}{f_2 - f_1}\left(n_2 - n_1 + \frac{\varphi_2 - \varphi_1}{2\pi}\right), \end{aligned} \tag{3}$$

where $\Delta n = n_2 - n_1$ is the difference in the number of cycles n_i accrued by frequency f_i. Ambiguity occurs when $\Delta n \neq 0$; in this case when $t_F > \Delta f$. Therefore, using multi-frequency signals allows a TOF measurement related not to the frequency of any signal, but the difference between the frequencies of two signal components.

This method is illustrated in Fig. 2, and can be intuitively understood by considering that two similar frequencies (say 40 and 41 kHz), when added together, will create a beating effect, where the amplitude of the signal will be modulated at a frequency of 1 kHz. Indeed, for any two signals $A\sin(\omega_1 t)$ and $A\sin(\omega_2 t)$, the sum can be expressed (through standard trigonometric identities) as $2A\cos(((\omega_2 - \omega_1)/2)t)\ \sin(((\omega_2 + \omega_1)/2)t)$. In combining two signals close in frequency for this phase measurement, one is effectively creating an artificial low-frequency signal (the modulation) that intrinsically has a longer unambiguous range derived from phase measurements (note, how-

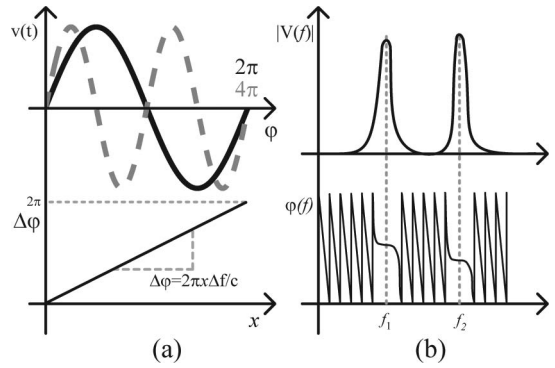

Fig. 2. Schematic of a two-frequency phase-based method. (a) A single-frequency signal of frequency f accrues 2π of phase in one cycle (black line, top), equivalent to a time $t_F = 1/f$. A signal at $2f$ will accrue 4π during the same distance (gray dashed line, top). The difference between the two phases $\Delta\phi$ (bottom) obeys the equation $\Delta\phi = 2\pi x\Delta f/c$, where Δf is the difference in the two frequencies. (b) A received two-frequency ranging signal in the Fourier domain. There will be two peaks in the magnitude of the spectra (top), and correspondingly, two phases at these peaks (bottom). The difference in these phases can be used to calculate the time-of-flight.

ever, that it will not suffice simply to measure the phase of the envelope because this signal is overmodulated).

Perhaps the clearest advantage to this method is when one is restricted to the use of relatively narrowband transducers. A slow amplitude-modulated signal effectively comprises two signals close in frequency that would fall within the bandwidth of the transducer. There are some disadvantages however. First, to extend the unambiguous range of this method, the frequency resolution (or bin width, where the frequency bin width df relates to the total length of the time-series data T by $df = 1/T$) must be minimized in the Fourier transform (such that closely spaced frequencies, which directly relate to the length of the time series sampled, can be resolved). It should be noted that this restriction only applies to Fourier transform methods of extracting phase, and there exist other high-resolution spectral-estimation tools that may avoid this problem. Second, a reasonable number of cycles should be present in the time-series data so that the information at the relevant frequencies is robust with respect to noise, i.e., long transmitted pulses are required. Thus, a disadvantage to this method is that, in a complex acoustic environment, closely spaced echoes (or multiple paths between transmitter and receiver) may be unresolvable, and, in fact, multiple echoes that overlap will result in an inaccurate measurement of the phases of received signals.

It is, of course, possible to extend this technique to any number of discrete frequencies in a signal. Because the unambiguous range for a particular two-frequency measurement is inversely proportional to the difference in those two frequencies, one can use, say, three well-chosen frequencies to improve a TOF measurement. With 3 frequencies there are 3 two-frequency pairs, and it is possible to choose two very similar frequencies and one very different one. In this case, the two close frequencies are used to calculate a first estimate of t_F, followed by a more refined estimate based on, say, the first and third frequency. Details can be found in [23]–[25] and references therein. Typical values for accuracy error can be seen in [23], which quotes an uncertainty in their experiment from temperature, humidity, and phase shift, of 0.26 mm for a measurement of between 500 mm to 3000 mm.

A multi-frequency phase technique for measuring the TOF is suitable for narrowband transducers, because the frequencies chosen can usually fit within the bandwidth of the transducer. However, care must be taken for correct calibration—narrowband transducers, as resonators, tend to have rapidly changing phase responses as a function of frequency. When one calculates the relative phase between the two frequencies, any additional phase shift caused by the transducer response will introduce error. This can be seen in Fig. 3(inset) in a different context. The dotted curve is the relative phase response of a broadband signal through a hypothetical transducer in a pitch–catch experiment. The true TOF t_F is found from the gradient of the gray line, that is, $2\pi t_F = \mathrm{d}(\Delta\phi)/\mathrm{d}f$. However, the relative phase differences between f_1, f_2, and f_3 are biased, and do not accurately indicate the true gradient.

C. Chirps and the Cross-Spectrum

Having transducers with increased bandwidth allows access to other ranging techniques which are reliant ultimately on the method of cross-correlation and its Fourier-domain counterpart, the cross-spectrum. Wideband signals can be pulse-compressed with cross-correlation, increasing the accuracy of the measurement, with the additional benefit of increasing the ability to resolve echoes (Fig. 3, where a multi-path chirp waveform is unresolvable, but after cross-correlation, peaks a, b, and c are easily resolved), and they therefore offer an attractive way to handle multi-path signals. A wideband chirp essentially provides an extension of the multi-frequency phase technique: a change from discrete frequency operation to continuous frequency representation. This is apparent by noting that (3) is a simple case of a more general equation that describes the behavior phase as a function of frequency and its relation to the TOF of an acoustic pulse. In the limit of $\Delta f \to 0$, with $\Delta n = 0$, (3) becomes

$$t_F = \lim_{\Delta f \to 0}\left(\frac{1}{\Delta f}\frac{\Delta\varphi}{2\pi}\right) = \frac{1}{2\pi}\frac{\partial\varphi}{\partial f}, \tag{4}$$

which is a general result relating the TOF $t_F = x/c$ to the gradient of a relative phase versus frequency plot. Therefore, with a wideband signal, one only needs to know the relative phase between the two signals over a range of frequencies to obtain a value for the TOF.

The easiest way to calculate the relative phase between two chirped signals is by calculating the cross-spectrum. Recall that for a transmitted and received signal [$s_T(t)$ and $s_R(t)$, respectively], the cross-spectrum is $C(f) = \mathcal{F}(c(t)) = S_T^*(f)S_R(f)$, where $c(t)$ is the cross-correlation of $s_T(t)$ and $s_R(t)$, and $S_T(f)$ and $S_R(f)$ are their Fourier

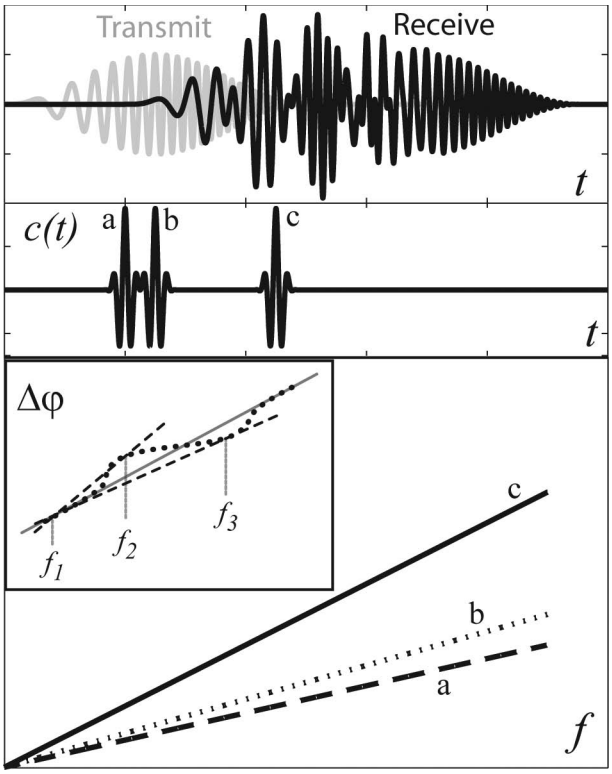

Fig. 3. Schematic diagram of the phase-spectrum method to calculate t_F for multiple overlapping echoes. (top) Multiple echoes overlapping in the received signal. (middle) Cross-correlation $c(t)$ reveals the presence of three distinct echoes (a, b, and c). (bottom) Three relative phase versus frequency plots can be calculated from each peak individually—the gradients of each line correspond to the time-of-flight t_F. If one were to use the entire received signal instead of the individual echoes, the resulting graph is very similar to line b. (inset) Transducer properties can introduce variation in the expected linear trend—the dotted black line is an exaggerated phase response.

transforms. The phase of the cross-spectrum is $\arg(C(f)) = \arg(S_T^*(f)S_R(f)) = \arg(S_R(f)) - \arg(S_T(f))$; that is, the phase of the cross-spectrum is the difference in the phases between received and transmitted signal.

A phase-based measurement of a chirp can therefore be performed by calculating the cross-spectrum $C(f)$ between the transmitted and received signals. The relative phase $\Delta\varphi_C$ is obtained through $\Delta\varphi_C = \tan^{-1}(\Im(C(f))/\Re(C(f)))$, where $\Im$ and $\Re$ are the imaginary and real parts, respectively. This relative phase must be unwrapped to reveal a linear relative phase as a function of frequency. At this point, a simple linear fit will give the value of $d\varphi/df$ to be used in (4) to calculate the TOF t_F of the acoustic signal. This method is illustrated in Fig. 3.

The type of transducer available dictates whether this method is useful. However, should one have the capability, this method is an improvement on cross-correlation because it is not restricted to the sampling of the true cross-correlation, and it does not rely on any curve fitting, such as parabolic fitting to the cross correlated peak (e.g., [20]). Rather than trying to pick a peak of one sample, or fit to a peak of three points, in the temporal domain, this method moves to the Fourier domain, where the linear phase behavior can be fitted and, in a sense, averaged (e.g., Fig. 4). Furthermore, extra processing makes this technique very powerful. Cross-correlation, as noted before, compresses the signal such that overlapping echoes are more easily separable (Fig. 3). Coupled with this is the knowledge of the initial transmitted signal, and therefore the theoretical width of the pulse when cross-correlated (Fig. 3, where three overlapping echoes are separated). With this information, the algorithm can be further enhanced by performing cross-correlation, detecting a peak corresponding to an echo, zeroing out every data point except the signal of interest (using the theoretical width as a guide to which data to retain), and then proceeding to the Fourier domain as outlined before. The gradient of the phase of each cross-spectrum indicates the TOF. Using this method, one can perform this technique on multiple overlapping echoes [Fig. 3—each cross-correlated peak (a, b, and c) has a different gradient in a graph of the relative phase versus frequency], which, although not directly relevant to the problem of 1-D TOF measurements, is an important additional benefit of this technique. Of note here is, in the data used for Fig. 3(bottom), a calculation of the relative phase of the whole received signal (comprising three echoes) gives a phase response versus frequency almost identical to line b in the bottom panel, effectively ignoring the first echo.

This phase-based method also reduces the effect of unknown frequency-dependent phase shifts caused by the transducer, or the measurement system [Fig. 3 (inset)] by averaging out any variation in phase that is not a trend. As discussed previously, methods such as the multi-frequency discrete phase-based method are susceptible to these errors and need calibration (Fig. 3).

Although a simple technique for separating echoes is to identify peaks in the cross-correlated data, and perform the phase-based Fourier method described previously on each individual pulse, there is another method involving the fractional Fourier transform [26]. In essence, overlapping echoes can be separated by rotating the frequency-

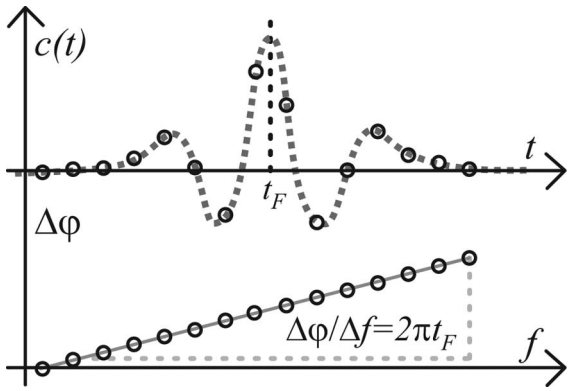

Fig. 4. Undersampling. (top) Cross-correlation, where the gray dotted line is the true curve, and the circles represent sampled data points. (bottom) In the Fourier domain. Although only one data point is used temporally to find t_F (or a few if using a curve-fitting algorithm), all samples across the relevant frequency range are used in the Fourier domain—thus a straight line fit to the phase versus frequency trend is more robust.

time domain onto a new frame of reference in which the echoes no longer overlap in a new time variable. In this case, a phase-based method to calculate TOF combined with the fractional Fourier transform method could be very powerful.

As an aside, it is interesting to note that the unambiguous temporal range criterion, which limits the difference between two frequencies chosen for the two-frequency ranging method, is still present in the linear-chirp phase-based method. In the latter case, however, this frequency difference is the spectral resolution (bin width) of the FFT performed and exists because ambiguity will occur when unwrapping the phase of the cross-spectrum should the phase increase faster than 2π per bin. For example, if the distance being measured in a ranging application is 1 m, the relative phase obeys the equation $\phi = 2\pi xf/c \sim 0.018f$. Phase wrapping occurs every 2π, so wrapping will occur in this case every $f = 345$ Hz. Bin widths larger than this value will unwrap incorrectly, underestimating the distance by 1 m, or an integer multiple of it. This problem is easily addressed by recording data for longer (or zero-padding). To achieve a 345 Hz bin width or less, one must record for ~3 ms.

D. Comparison of Phase/Cross-Spectrum Ranging to Cross-Correlation

Although there are many studies on the errors (whether in accuracy or in repeatability) for thresholding, and some for multi-frequency phase ranging, to the authors' knowledge, there is no study on the accuracy or repeatability of the phase/cross-spectrum method. For this reason, a preliminary study was conducted into how the phase/cross-spectrum method performs as a ranging technique in air against cross-correlation for various distances as a function of sampling frequency (Fig. 5). A chirp of 20 to 120 kHz was transmitted from a custom-made wideband capacitive ultrasonic transducer (with a bandwidth of 20 to 600 kHz) to a calibrated microphone [4138, 3.175-mm (1/8-in), Bruel and Kjaer, Naerum, Denmark] placed at various distances on the acoustic axis of the transducer. The microphone itself was placed on a linear encoder with a positioning accuracy of 250 μm, over a range of 10 to 90 cm. For each distance, 10 single-shot chirps were recorded, and the distance calculated using both the phase/cross-spectrum method and cross-correlation, to determine the repeatability of each method.

One of the main strengths of the Fourier domain phase/cross-spectrum method was its robustness with respect to sampling frequency, resulting from the inherent form of interpolation in the linear fit. Fig. 5 shows the accuracy and repeatability of the phase/cross-spectrum method and cross-correlation for sampling frequencies of 20 MHz and 500 kHz. Note that 500 kHz is approaching Nyquist's limit for the higher frequencies in the chirp. Although both methods are equally accurate, with an error less than 400 μm (in this case measured as the difference between the mean of 10 measurements and the real value), the re-

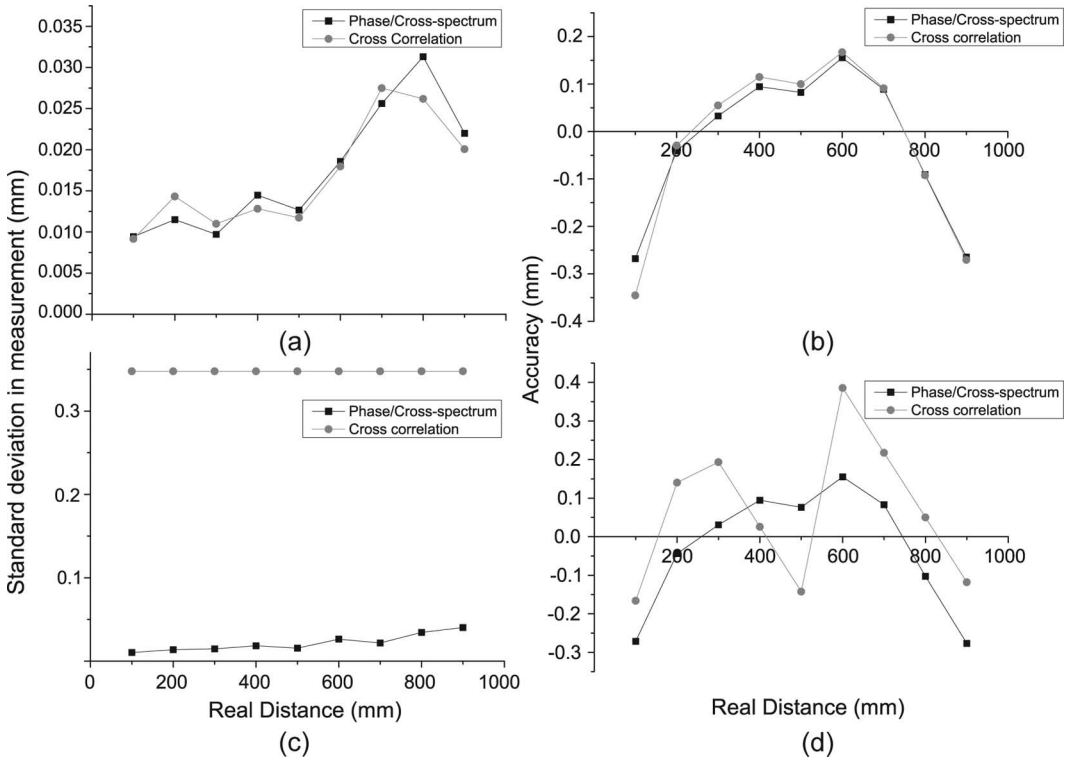

Fig. 5. Comparison of the accuracy (difference of the mean from the real value) and repeatability (standard deviation of 10 repeated measurements) of both the phase/cross-spectrum method and cross-correlation as a function of distance from transmitter to receiver. (a) and (b): A 20 to 120 kHz chirp sampled at 20 MHz. (c) and (d): A 20 to 120 kHz chirp sampled at 500 kHz (approaching Nyquist's limit for higher frequencies in the chirp).

peatability is affected notably by the sampling frequency. The phase/cross-spectrum method maintains a repeatability of sub-30 μm at a sampling frequency of 500 kHz, whereas cross-correlation is limited by the reduced temporal resolution and can only provide ~350 μm resolution.

Reducing the sampling frequency is an excellent way to reduce the computational requirements of any ranging method. The phase/cross-spectrum method, therefore, allows one to profit from the advantages of wideband cross-correlation methods, such as the increased resolution of overlapping echoes and noise reduction, while utilizing a reduced sampling frequency to improve speed of computation and to maintain an excellent repeatability.

For completeness, Fig. 6 is a comparison of the repeatability (standard deviation of 10 repeated measurements) of both the phase/cross-spectrum method and cross-correlation as a function of distance from transducer to microphone. The solid lines are the measured data, the SNRs of which, measured at 100 and 900 mm, are 35 and 19 dB, respectively. To this data, Gaussian noise has been added to give SNRs of 19 and 3 dB, respectively (dashed lines), and 13 and 1 dB, respectively (dotted lines). When sampled at 20 MHz, both methods have sub-30 μm repeatability, although increasing noise clearly affects the phase/cross-spectrum repeatability more than it does cross-correlation. When the signals are sampled at only 500 kHz, the undersampling causes the repeatability of the cross-correlation to be poor, again as the lack of resolution dominates. Noise clearly affects the phase/cross-spectrum method in undersampling contexts too, but can still beat the resolution problem for small distances. Note that although noise is added to the signals post-capture, increasing distance also decreases the SNR.

IV. Hybrid Models

Hybrid methods incorporating both temporal and frequency-domain information have also been described (e.g., [20], [27]). In these methods, one calculates a first estimate of delay through cross-correlation (or even simple thresholding), followed by a fine measurement of the phase of a frequency component. This method can be used to exploit situations in which hardware specification is unavoidably poor, for example, in autonomous ranging [27]. The first TOF measurement is often rendered less accurate should one be restricted to low-sampling-rate hardware. However, one can calculate the number of cycles an acoustic wave has accrued from this measurement. In the frequency domain, the phase of a frequency component can then give a more accurate interpolation of the true TOF [27]. Other ways of calculating the phase include sine-fitting techniques [20]. In this study, using a sine-fitting technique can produce errors in distance measurement of ~300 μm (accuracy) and ~7 to 60 μm (repeatability), which is significantly smaller than the typical wavelengths of ultrasound in air.

As with all discussed methods, the goal is to perform accurate TOF measurements while minimizing cost and maximizing practicality. Hybrid models of this type require modest digital signal processing, and as technology improves, at decreasing cost.

A. Biologically Inspired Ranging Algorithm

A previous study at the University of Strathclyde [29] has described a hybrid, biologically inspired algorithm that aims to mimic echolocation performed by bats. These animals have a preternatural ability to distinguish absolute and relative positions of ensonified objects in their acoustic environment [29], although the exact mechanism for their ability is unclear. The accuracies claimed for bats have led researchers to investigate ranging techniques based on models of bat hearing. The Biologically Inspired Ranging Algorithm (BIRA) was developed to exploit the accuracy and precision of bat echolocation [28].

Bats employ complex airborne ultrasonic chirp sequences enabling detection of sub-millimeter targets.

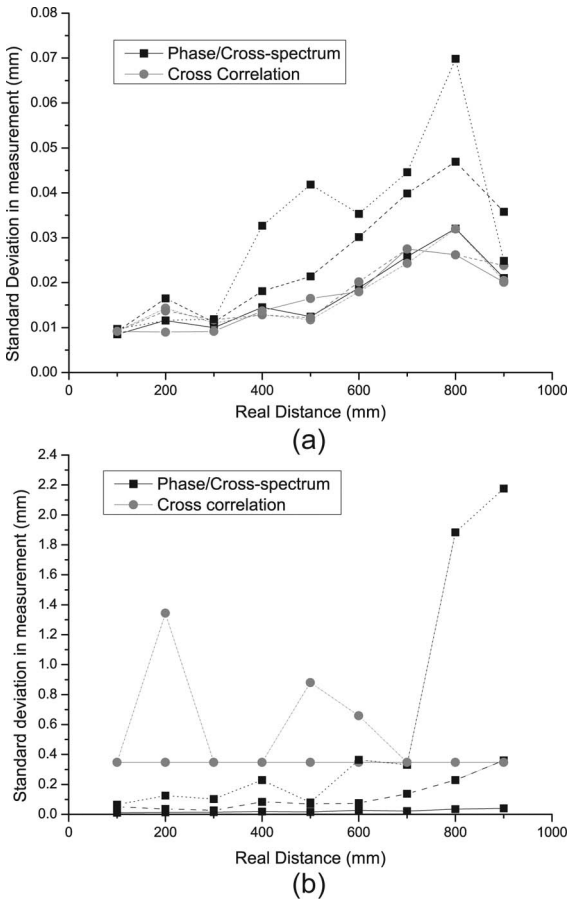

Fig. 6. Comparison of the repeatability (standard deviation of 10 repeated measurements) of both the phase/cross-spectrum method and cross-correlation as a function of distance from transmitter to receiver. The solid lines are the measured data, the SNR of which, measured at 100 and 900 mm, are 35 and 19 dB, respectively. To this data, Gaussian noise has been added to give SNRs of 19 and 3 dB, respectively (dashed lines), and 13 and 1 dB, respectively (dotted lines). (a) Sampled at 20 MHz. (b) Sampled at 500 kHz.

They display an impressive ability to discriminate closely spaced overlapping echoes in the received signal—it has been shown experimentally [29] that bats are able to resolve separation delays smaller than the inverse bandwidth limit imposed by man-made systems based on coherent matched filtering receivers [30]. The *Eptesicus fuscus* bat can discriminate echoes in air with a resolution of 2 μs versus 10 μs for conventional systems, assuming a signal bandwidth of 100 kHz. It is believed that the sonic emissions potentially composed of multiple spectral components and the associated signal processing of such signals enable this high-resolution discrimination. The underlying assumption is that bats possess this ability to identify the acoustic signature of their prey [29].

BIRA, developed by Devaud *et al.* [28], based upon the previous computational models by Matsuo *et al.* [31] and Saillant *et al.* [32], attempts to replicate, through time/frequency processing, the resolution with which bats are able to echolocate. BIRA processes a received signal $x_{\text{rec}}(t)$ that is composed of a sum of overlapping linear frequency-modulated (LFM) chirps inspired by bat signals. This signal is processed temporally to extract TOF while the *fine* delays arising from reflections, or glints, of the complex reflecting object are determined through frequency-domain processing. It is the temporal processing that is the focus of this section; see [28] for details of the fine delay extraction algorithm.

B. Temporal Processing

The temporal processing component of BIRA seeks to mimic the operation of the basilar membrane, a component of the bat inner ear. This membrane transforms received acoustic vibrations into electrical signals, where this conversion is a function of varying frequency sensitivity along the length of the membrane. The temporal block makes use of a filter bank as a first-order approximation of the basilar membrane [32]. The nature of the sweep function in real bat chirps varies among species but in general assumes a hyperbolic shape in time. LFM chirps were chosen as an engineering simplification, however, the temporal subsystem can be reconfigured to process more realistic sweep functions. The received signal $x_{\text{rec}}(t)$ is convolved with a filter bank composed of 101 Gaussian chirplet filters characterized by the following equation [31]:

$$F(f_j,t) = \exp\left(\frac{-t^2}{\alpha}\right)\exp\left(2\pi i\left(f_j t + \frac{1}{2}st^2\right)\right), \qquad (5)$$

where f_j is the starting frequency for the jth chirplet filter, s is the sweep rate of the emitted wave, and α is a parameter for the width of the Gaussian window function. The filter bank serves to decompose the received signal into a set of sub-bands, each appearing in time as function of the linear frequency modulation, an effect similar to the action of the mammalian cochlea. The computational complexity of the algorithm is quadratic in the number of filters, N, and therefore the selection of 101 filters represents a compromise between an efficient discretization of the bandwidth and a manageable computational complexity, following the model of Matsuo *et al.* [31].

The action of the temporal block can be viewed as an approximate parallel form of cross-correlation wherein the signal is simultaneously convolved with several filters, each of which processes a particular spectral band of the input. It is essentially carrying out a cross-correlation of the received signal with a discretized version of the transmitted chirp—the action of the temporal block is illustrated in Figs. 7(a) and 7(b). The TOF information is extracted through aligning the outputs of the filter bank with respect to the frequency which occurs first in time. The sum of the filter outputs across the time axis is then evaluated, resulting in a single waveform, the maximum peak of which is taken to be the TOF of $x_{\text{rec}}(t)$. This process is illustrated in Fig. 7(c), where a subset of filter bank outputs is shown and subsequently aligned and summed to produce the single waveform used to estimate TOF.

The performance of BIRA was compared with the phase/cross-spectrum method and cross-correlation presented in Section III-D. Fig. 7(d) shows the result of repeatability as a function of distance. As can be seen, the standard deviation is sub-millimeter and displays a similar performance to the cross-spectrum technique.

V. Limitations on Accuracy

If the distance between a transmitter and a receiver in air is to be calculated, rather than the TOF, there is a large source of error arising from the speed of sound in the medium. Unlike optical (or radio) techniques for measuring the time of arrival of a pulse, the speed of sound is strongly dependent on temperature. Treated as an ideal gas, the speed of sound in air c is given by

$$c = \sqrt{\frac{\gamma p}{\rho}} = \sqrt{\frac{\gamma RT}{M}}, \qquad (6)$$

where γ is the adiabatic index of air, p is the pressure, and ρ is the density. Eq. (6) can be approximated to $c = 300 + 0.6\,T(^{\circ}\text{C})$ where T is now in degrees Celsius. For an ideal gas, the pressure $p = \rho RT/M$ has been included to give a value for the speed of sound independent of pressure but dependent on the ideal gas constant R, the molar mass M, and the ambient temperature T (in Kelvin). Note that (6) is derived under the assumption of air behaving as an ideal gas, and is therefore still an approximation. Following from (6), the fractional error in a range measurement $\Delta d/d$ (where Δd is the standard deviation, or error, of the range measurement d) can be calculated as a function of the fractional error in both TOF $\Delta t_{\text{F}}/t_{\text{F}}$ and temperature $\Delta T/T$ using

$$\left(\frac{\Delta d}{d}\right)^2 = \left(\frac{\Delta t_{\text{F}}}{t_{\text{F}}}\right)^2 + \frac{1}{4}\left(\frac{\Delta T}{T}\right)^2. \qquad (7)$$

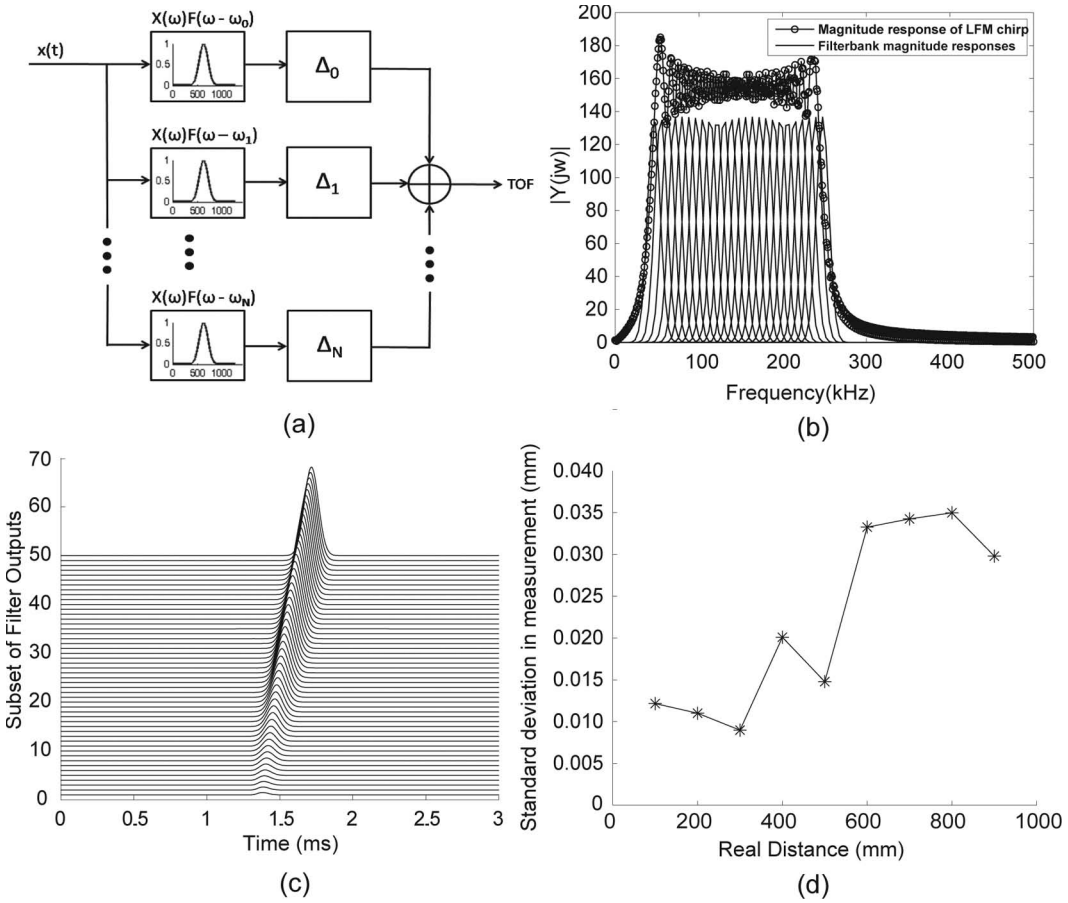

Fig. 7. (a) Block diagram of the temporal block. The input signal $x_{\text{rec}}(t)$ is convolved with a filter bank composed of 101 Gaussian chirplet filters, the resulting outputs are aligned in time with respect to the signal frequency component which occurs first in time. The time-of-flight is then taken to be the maximum of the sum of the compensated outputs. (b) The filters composing the filter bank process different frequency bands across the spectral occupancy of the input chirp signal. (c) The received Hann windowed chirp is converted into a series of pulses, of which a subset of the filter bank outputs is shown. The linear trend corresponds to the linear sweep rate of the chirp. (d) Standard deviation in 10 repeated measurements versus distance. In this case, the sampling frequency is 20 MHz.

Ignoring the potential errors in the molar mass M and the ideal gas constant R, (7) illustrates the difficulty in obtaining accuracy in many practical scenarios. In (7), the fractional error derived from an uncertain temperature can be far greater than the fractional error in the TOF measurement; the fractional error in distance would be dominated by the temperature inaccuracy. In this case, the fractional error in a range measurement behaves linearly with respect to the fractional error in temperature ($\Delta d/d \sim \Delta T/2T$). Fig. 8 shows the behavior of (7), plotting the error in distance as a function of the error in temperature (at room temperature) for ranging measurement over 10 cm and 1 m. Fig. 8 also includes shading that illustrates the effect of the error in the TOF measurement. At a distance of 1 m (and for larger distances), the error in temperature is the dominant parameter, and there is little change in the total error in distance should the error in the TOF be reduced. An error of ~1 mm occurs for temperature uncertainties in the region of low-cost commercial temperature sensors (although with improved technology one can approach errors of sub-500 μm). For shorter distances (say, 10 cm), the TOF error becomes comparable in magnitude to the temperature error, and accuracy can be increased through improvements in the TOF measurement.

With the dominant error arising from temperature inaccuracy in any ultrasonic ranging system at long range (for example, distances greater than 1 m), elaborate algorithms for distance ranging in these conditions can be avoided, and thresholding would probably suffice, because there will be a bias in any measurement performed. There are methods for temperature-compensated ranging, almost entirely based on some direct temperature measurement and use of either (6) or the Taylor-series approximation of it. Thermistors and resistance temperature detectors, for example, can be used to provide a temperature-dependent voltage [33], and as technology improves, one can find reasonably priced sensors with a rated accuracy of around ~0.1° or better. If there are temperature gradients in the acoustic medium, however, then further problems exist, and accuracies decrease still further. For the reader's information, calculations made by Huang *et al.* [23] indicate that temperature uncertainty contributes 65% of their total distance measurement uncertainty using the multifrequency phase technique.

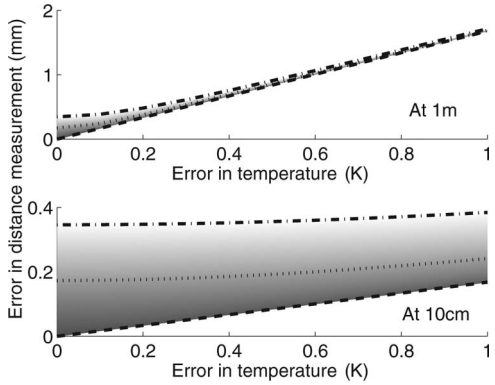

Fig. 8. Graph of the error in a distance measurement as a function of temperature uncertainty. The shading represents the effect of a time-of-flight error on this distance error; in these cases, black-to-white shading indicates the range of time-of-flight error of 0 μs (bounded by the dashed line) to 1 μs (bounded by the dot-dashed line). A time-of-flight error of 500 ns is indicated by the dotted-line contour. (top) A signal that has traveled 1 m in air. (bottom) A signal that has traveled 10 cm in air.

In practice, the only sure method of reducing the uncertainty in the speed of sound is to measure it directly. Removing completely the need for an accurate temperature measurement, Chande *et al.* [34] described a method of simply measuring the TOF of an acoustic pulse over a known distance while simultaneously insonifying the environment. This method independently measures the speed of sound of the medium, assuming this known distance is accurately measured. The fractional error in a range measurement for this method is simply the Pythagorean sum of the fractional errors in the TOFs and the known distance. This compensation therefore now relies on an accurate TOF measurement over the known distance. Hence, when the speed of sound can be satisfactorily compensated, the accuracy and repeatability of the TOF measurement dictate the performance of a ranging system.

VI. Conclusions and Discussion

The selection of an appropriate method for through-air ultrasonic ranging depends upon several factors including cost, ease of implementation, technical requirements, and the local environment.

Detailed comparative performance figures for the various methods described previously can be found in Table I. The majority of the results in this table arise from experiments performed specifically for this paper (indicated by a double dagger in Table I), although there are some external sources of information. Experiments done by the authors were through-air pitch–catch tests. Accuracy and repeatability are collated for the following methods: simple thresholding (Th), cross-correlation of a pulse (CC), cross-correlation of linear chirps (FM-C), multi-frequency phase-based measurement (MFP), phase spectrum method (PS), and BIRA. The domain is indicated to be a temporal, Fourier-based, or a hybrid method. The source of the data for each method is indicated, and where possible, the SNR over which the accuracies and repeatabilities are valid.

For experiments performed specifically for this paper, the data was gathered in the same way as for the phase/cross-spectrum method detailed previously (10 repeat measurements of a pitch–catch experiment between two custom-made wideband transducers were made at various distances between 10 and 90 cm). The quoted SNR was calculated for real data and adding simulated noise (Gaussian white noise) such that the SNR were comparable to the values quoted in [13]. The three external sources of information quoted in Table I all effectively performed the same type of measurement (pitch–catch), with only minor differences in procedure. For example, [13] uses a 40-kHz narrowband transducer and no wideband transducers.

First, it is clear from Table I that of the temporal methods described, cross-correlation of a pulse (CC) or a chirp (FM-C) can give sub-millimeter accuracy and repeatability. From our work, it is known that cross-correlation of a chirp can give sub-millimeter figures for SNR values in the 0 to 35 dB range. The repeatability quoted as <0.03 mm is approaching the theoretical limit dictated by the temporal resolution (in this case, the sampling frequency was 20 MHz, which equals a spatial resolution of ~9 μm). The thresholding method suffers from bias, as

TABLE I. Comparison of the Accuracy and Repeatability of Different Ranging Algorithms.

Method	Domain	Accuracy (mm)	Repeatability (mm)	SNR (dB)	Source
Th	Time	~6	~0.8	35	[13]
Th	Time	~5	~5	—	‡
CC	Time	~2	~1	—	[20]
CC	Time	~0.004	~0.185	35	[13]
FM-C*	Time	<0.400	<0.030	0 to 35	‡
MFP	Frequency	0.260	—	—	[23]
MFP	Frequency	<0.300	<0.015	~35	‡
MFP	Frequency	~1	~1	~6	‡
PS*	Frequency	<0.400	<0.010	~35	‡
PS*	Frequency	<0.400	<0.070	~0	‡
BIRA	Hybrid	<0.350	<0.015	~35	‡
BIRA	Hybrid	<0.300	<0.040	~0	‡

TABLE II. REQUIREMENTS OF EACH METHOD.

Method	Bandwidth	Comp. cost	SNR (dB)	f_s
Th	N/A	Low	>35	>1 MHz
CC	N/A	Moderate	~15	>1 MHz
FM-C*	20 to 250 kHz	Moderate	~−13	>5 MHz
MFP	c/R	Moderate	~6	>1 MHz
PS*	20 to 250 kHz	Moderate	>−1	500 kHz
BIRA	20 to 250 kHz	High	>3	500 kHz

expected, with an accuracy of 6 mm at 35 dB SNR. The Fourier-domain methods, in general, perform better. Accuracies of <0.5 mm exist for 0 to 35 dB SNR, and the repeatability of these methods is below 100 μm. Only the multi-frequency phase method loses accuracy for decreasing SNR—indeed, below 6 dB SNR, we found that the method became unstable. BIRA performs at the level of cross-correlation and the phase-spectrum method, highlighting the similarities in their methodologies.

As a final point, most methods lose accuracy and repeatability as the sampling frequency is decreased toward Nyquist's limit: Methods marked with asterisks in Table I are methods that still retain quoted accuracies in this limit.

Table II is a summary indicating the authors' opinion on the suitability of each method for any application. This table shows the transducer bandwidth required for the method, the computational cost (which will affect speed), and the minimum sampling frequencies we believe should be used to ensure accuracy. The minimum SNR is calculated with simulated noise on real data (additive white noise for the asterisked methods; noise used for the other methods can be found in the references indicated in Table 1), and we quote values that indicate a 1-mm repeatability at the given sampling frequency f_s. It is important to note that sampling frequency and SNR are not independent in their effect on the repeatability, and it is possible to increase the minimum SNR needed by increasing the sampling frequency, particularly for Fourier-domain methods such as the phase/cross-spectrum method.

Thresholding is usually a narrowband method, and can be achieved with simple analog circuitry, but is susceptible to noise. Cross-correlation is considered optimal—narrowband signals cannot be compressed however, so echo separation is still poor. The multi-frequency phase method (MFP) is a narrowband method as well, and the required bandwidth is c/R, where c is the speed of sound in air, and R is the unambiguous range desired. This method can perform well in low SNR, but again echoes can interfere with the result. None of the temporal methods or the MFP method performs well under low sampling conditions. Of the wideband methods, the phase-spectrum method and BIRA perform well under all conditions, but require more computation and, of course, require wideband transducers. Furthermore, for an individual frequency, wideband transducers output a lower sound pressure than narrowband transducers, so care must be taken to ensure that attenuation is considered. The values quoted for the bandwidth in Table II reflect the range in which sound is both inaudible and not highly attenuated in air. For the sampling frequency, a value is quoted relating either to a 40-kHz narrowband transducer or a generic wideband transducer. The reader should balance the accuracies and repeatabilities for each method in Table I with their constraints indicated in Table II.

Although we are only concerned with through-air ranging applications, this review and study, and the methods and concepts, are extendable to different fields of engineering that require a measurement of the TOF of a signal. In summary, this article has discussed various methods for measuring the TOF of an acoustic pulse for through-air applications. Limiting factors such as technological constraints, or fluctuating ambient temperatures, dictate which method is most suitable for an application. In the context of distance ranging in air, sub-500 μm accuracy is possible in air under certain circumstances, and the repeatability of some of the discussed algorithms can approach 10 μm.

REFERENCES

[1] M. Friedrich, G. Dobie, C. C. Chan, S. G. Pierce, W. Galbraith, S. Marshall, and G. Hayward, "Miniature mobile sensor platforms for condition monitoring of structures," *IEEE Sensors J.*, vol. 9, no. 11, pp. 1439–1448, 2009.

[2] N. B. Priyantha, H. Balakrishnan, E. D. Demaine, and S. Teller. "Mobile-assisted localization in wireless sensor networks," in *Proc. IEEE INFOCOM* 2005, vol. 1, pp. 172–183.

[3] J. Hightower and G. Borriello, "Location systems for ubiquitous computing," *Computer*, vol. 34, no. 8, pp. 57–66, 2001.

[4] R. K. Harle and A. Hopper, "Building world models by ray-tracing within ceiling-mounted positioning systems," *Lect. Notes Comput. Sci.*, vol. 2864, pp. 1–17, 2003.

[5] Vicon http://www.vicon.com

[6] E. Kaplan and C. Hegarty, *Understanding GPS: Principles and Applications*, 2nd ed., Norwood, MA: Artech House, 2006.

[7] Leica-Geosystems http://metrology.leica-geosystems.com/en/index.htm

[8] N. B. Priyantha, A. Chakraborty, and H. Balakrishnan, "The cricket location-support system," in *Proc. MOBICOM 2000*, pp. 32–43.

[9] S. Thrun, "Probabilistic robotics," *Comm. ACM*, vol. 45, no. 3, pp. 52–57, 2002.

[10] *URG-04LX Datasheet*. Hokuyo Automatic Co. Ltd., Osaka, Japan, 2005.

[11] Y. Okubo, C. Ye, and J. Borenstein, "Characterization of the Hokuyo URG-04LX laser rangefinder for mobile robot obstacle negotiation," *Proc. SPIE*, vol. 7332, art. no. 733212, 2009.

[12] R. Halmshaw, *Non-Destructive Testing*. London, UK: Edward Arnold, 1997.

[13] B. Barshan, "Fast processing techniques for accurate ultrasonic range measurements," *Meas. Sci. Technol.*, vol. 11, no. 1, pp. 45–50, 2000.
[14] B. Barshan and R. Kuc, "A bat-like sonar system for obstacle localization," *IEEE Trans. Syst. Man Cybern.*, vol. 22, no. 4, pp. 636–646, Jul./Aug. 1992.
[15] G. Benny, G. Hayward, and R. Chapman, "Beam profile measurements and simulations for ultrasonic transducers operating in air," *J. Acoust. Soc. Am.*, vol. 107, no. 4, pp. 2089–2100, 2000.
[16] M. Parrilla, J. J. Anaya, and C. Fritsch, "Digital signal processing techniques for high accuracy ultrasonic range measurements," *IEEE Trans. Instrum. Meas.*, vol. 40, no. 4, pp. 759–763, Aug. 1991.
[17] W. G. McMullan, B. A. Delaughe, and J. S. Bird, "A simple rising-edge detector for time-of-arrival estimation," *IEEE Trans. Instrum. Meas.*, vol. 45, no. 4, pp. 823–827, Aug. 1996.
[18] S. W. Smith, *Digital Signal Processing: A Practical Guide for Engineers and Scientists*. Oxford, UK: Newnes, 2003.
[19] D. Marioli, C. Narduzzi, C. Offelli, D. Petri, E. Sardini, and A. Taroni, "Digital time-of-flight measurement for ultrasonic sensors," *IEEE Trans. Instrum. Meas.*, vol. 41, no. 1, pp. 93–97, Feb. 1992.
[20] R. Queiros, P. S. Girao, and A. Cruz Serra, "Cross-correlation and sine-fitting techniques for high resolution ultrasonic ranging," in *Proc. IEEE Instrumentation and Measurement Technology Conf.*, 2006, pp. 552–556.
[21] J. A. Simmons, "A view of the world through the bat's ear: The formation of acoustic images in echolocation," *Cognition*, vol. 33, no. 1–2, pp. 155–199, 1989.
[22] C. F. Moss and H.-U. Schnitzel, "Accuracy of target ranging in echolocating bats: Acoustic information processing," *J. Comp. Physiol. A*, vol. 165, no. 3, pp. 383–393, 1989.
[23] K.-N. Huang and Y.-P. Huang "Multiple-frequency ultrasonic distance measurement using direct digital frequency synthesizers," *Sens. Actuators A*, vol. 149, no. 1, pp. 42–50, 2009.
[24] W.-Y. Tsai, H.-C. Chen, and T.-L. Liao, "High accuracy ultrasonic air temperature measurement using multi-frequency continuous wave," *Sens. Actuators A*, vol. 132, no. 2, pp. 526–532, 2006.
[25] S. Assous, C. Hopper, M. Lovell, D. Gunn, P. Jackson, and J. Rees, "Short pulse multi-frequency phase-based time delay estimation," *J. Acoust. Soc. Am.*, vol. 127, no. 1, pp. 309–315, 2010.
[26] D. M. J. Cowell and S. Freear, "Separation of overlapping linear frequency modulated (LFM) signals using the fractional Fourier transform," *IEEE Trans. Ultrason. Ferroelectr. Freq. Control*, vol. 57, no. 10, pp. 2324–2333, 2010.
[27] F. E. Gueuning, M. Varlan, C. E. Eugne, and P. Dupuis, "Accurate distance measurement by an autonomous ultrasonic system combining time-of-flight and phase-shift methods," *IEEE Trans. Instrum. Meas.*, vol. 46, no. 6, pp. 1236–1240, Dec. 1997.
[28] F. Devaud, G. Hayward, and J. J. Soraghan, "Evaluation of a biol.-inspired range finding algorithm (BIRA)," in *IEEE Ultrasonics Symp.*, 2006, pp. 1381–1384.
[29] J. Simmons, M. Ferragamo, C. F. Moss, S. B. Stevenson, and R. A. Altes, "Discrimination of jittered sonar echoes by the echolocating bat, *Eptesicus fuscus*: The shape of target images in echolocation," *J. Comp. Physiol. A*, vol. 167, no. 5, pp. 589–619, 1990.
[30] D. K. Barton and S. A. Leonov, *Radar Technology Encyclopedia*. Norwood, MA: Artech House, 1997.
[31] I. Matsuo, K. Kunugiyama, and M. Yano, "An echolocation model for range discrimination of multiple closely spaced objects: Transformation of spectrogram into the reflected intensity distribution," *J. Acoust. Soc. Am.*, vol. 115, no. 2, pp. 920–928, 2004.
[32] P. A. Saillant, J. A. Simmons, S. P. Dear, and T. A. McMullen, "A computational model of echo processing and acoustic imaging in frequency-modulated echolocating bats: The spectrogram correlation and transformation receiver," *J. Acoust. Soc. Am.*, vol. 94, no. 5, pp. 2691–2712, 1993.
[33] C. Canali, G. De Cicco, B. Morten, M. Prudenziati, and A. Taroni, "A temperature compensated ultrasonic sensor operating in air for distance and proximity measurements," *IEEE Trans. Ind. Electron.*, vol. IE-29, no. 4, pp. 336–341, Nov. 1982.
[34] P. K. Chande and P. C. Sharma, "A fully compensated digital ultrasonic sensor for distance measurement," *IEEE Trans. Instrum. Meas.*, vol. 33, no. 2, pp. 128–129, Jun. 1984.

Joseph C. Jackson received his M.Sci.(Hons.) degree in physics in 2003 from Imperial College, London. He then received his Ph.D. degree in biological sciences from the University of Bristol in 2008. He is currently at the Centre for Ultrasonic Engineering, University of Strathclyde, undertaking an EPSRC Cross-disciplinary Post-doctoral Fellowship in the study of animal hearing and its applications to bio-inspired sensors and actuators. His research interests cover a wide range of subjects, such as the physical basis for hearing, ultrasound production and reception in biology and engineering, biosonar, and advanced bio-inspired transducer and signal design.

Rahul Summan received the M.Eng. degree in computer and electronic systems from the University of Strathclyde in 2008. He is currently pursuing a Ph.D. degree in robotics, based in the Centre for Ultrasonic Engineering at the University of Strathclyde. He has research interests in the application of probabilistic techniques for robotic mapping, data fusion, and image processing.

Gordon Dobie is a Research Fellow in the Department of Electronic and Electrical Engineering at the University of Strathclyde. He received his M.Eng. degree in electrical and mechanical engineering from the University of Strathclyde and his Ph.D. degree from the Centre for Ultrasonic Engineering (CUE) developing a reconfigurable noncontact inspection system. His primary research interests include ultrasonics, NDE, automation, robotics, signal processing, computer vision, and embedded systems. His current work in the CUE focuses on the automated ultrasonic inspection of complex geometries.

Simon M. Whiteley is working with Alba Ultrasound in Glasgow as an Acoustic Design Engineer, designing high-end sonar arrays. He gained his Ph.D. degree with the Centre for Ultrasonic Engineering (CUE) at the University of Strathclyde, where his research activities focused on biosonar, bio-inspiration, and biomimetics, generally in the field of air-coupled ultrasound and its applications. He received his B.Eng.(Hons) degree from the Electronic and Electrical Engineering Department at the University of Strathclyde in 1996.

S. Gareth Pierce is a Senior Lecturer in Electronic and Electrical Engineering (EEE) at Strathclyde University, based in the Centre for Ultrasonic Engineering (CUE). He received his B.Sc.(Hons.) degree in pure and applied physics in 1989 and his Ph.D. degree in fiber optic applications to laser ultrasonics in 1993 from The University of Manchester, UK. He is the author of more than 40 peer-reviewed journal papers and has been involved with research into nondestructive evaluation (NDE) and structural health monitoring (SHM) since 1990. His work as part of the UK Research Centre in NDE (RCNDE) focuses on robotic inspection vehicles; in particular, the critical issues associated with accurate positioning and data presentation and fusion from multiple sensing methodologies. He sits on the management board of RCNDE and also on the International Scientific Committee for the European Workshop on Structural Health Monitoring.

Gordon Hayward is a research professor in the Department of Electronic and Electrical Engineering at the University of Strathclyde. He has been engaged in ultrasonics-related research for 25 years, with particular emphasis on the modeling and design of transducer and array systems for nondestructive testing, sonar, biomedical, and industrial processing applications. His research at Strathclyde has attracted external support from both government and industrial organizations, spanning the international community. He is also chairman of Alba Ultrasound Ltd., a company specializing in the manufacture of high-quality ultrasonic transducers and arrays.